Gas-Phase Reactions of Hydrocarbons with An^+ and AnO^+ (An = Th, Pa, U, Np, Pu, Am, Cm): The Active Role of 5f Electrons in Organoprotactinium Chemistry

John K. Gibson,*,† Richard G. Haire,† Joaquim Marçalo,*,‡ Marta Santos,‡ António Pires de Matos,‡ Michael K. Mrozik,§ Russell M. Pitzer,§ and Bruce E. Bursten⊥

Chemical Sciences Division, Oak Ridge National Laboratory, Oak Ridge, Tennessee 37831-6375, Departamento de Química, Instituto Tecnológico e Nuclear, 2686-953 Sacavém, Portugal, Department of Chemistry, The Ohio State University, 100 West 18th Avenue, Columbus, Ohio 43210, and Department of Chemistry, University of Tennessee, Knoxville, Tennessee 37996

Received April 4, 2007

Activation of small (C_1−C_4) alkanes and alkenes by bare and oxo-ligated actinide cations (Th^+ through Cm^+) has been systematically examined using Fourier transform ion cyclotron resonance mass spectrometry. The reduced reactivities of Pu^+, Am^+, and Cm^+ correlate with the energies for electronic excitation to a $5f^{n-2}6d7s$ configuration, which indicates that their 5f electrons are chemically inert. The reactivity trend identified for the highly reactive early actinide ions, $Th^+ > Pa^+ > U^+ > Np^+$, is interpreted to indicate significant 5f electron participation in organoactinide σ-type bond formation for Pa^+. Among the seven studied AnO^+ ions, only ThO^+, PaO^+, and UO^+ activated at least one hydrocarbon, with the reactivity of PaO^+ being distinctively high. Electronic structure calculations for PaO^+ show that its ground state is $Pa(5f6d)O^+$, i.e., with one 5f and one 6d nonbonding electrons available on the metal, and all of its excited states up to 1.8 eV have a 5f orbital occupancy of ≥0.8. The high reactivity and substantial 5f character of PaO^+ indicate participation of 5f electrons in hydrocarbon bond activation for oxo-ligated Pa^+. The results of this work reveal that 5f electrons play a distinctive role in protactinium chemistry involving σ-type organometallic bonding.

Introduction

Understanding the bonding of actinides with inorganic and organic ligands has long been a central theme of experimental and computational actinide chemistry.[1,2] The role of the quasi-valence 5f electrons/orbitals in molecular bonding is of special interest. Substantial 5f involvement in bonding has been established for several inorganic motifs, including the ubiquitous actinyls, AnO_2^{2+} (An = U, Np, Pu, Am).[3] In the realm of organoactinide chemistry, 5f participation in actinide−ligand bonding has been a central issue for systems such as uranocene[4,5] and other actinocenes,[6−8] where 5f orbital interactions with the π-electron systems of the cyclooctatetranyl ligands were historically thought to be key. Without excluding a secondary role for the 5f electrons, experiment[9] and theory[10] now indicate that the metal−ligand covalent bonding in uranocene is actually dominated by the 6d electrons. However, for σ-type organoactinide bonding, as in actinide alkyls, the 5f electrons are essentially uninvolved in bonding;[11] this latter class of σ-bonded organoactinides remains very limited in both breadth and the chemical stability of its members.[12] The issue of the role of 5f electrons/orbitals in bonding in actinide complexes has recently been discussed in detail by Bursten et al.[13]

Evaluation of the nature of bonding in organoactinides has traditionally been based primarily on structural and other physical properties of isolable condensed-phase complexes.[12,14] Early examinations of reactions of lanthanide ions (Ln^+) with hydrocarbons in the gas phase, by the groups of Freiser, Beauchamp, Armentrout, and Schwarz, have demonstrated the utility of this type of chemical reactivity in elucidating the role of electronic structures of 4f-element ions in inducing bond

* Corresponding authors. E-mail: gibsonjk@ornl.gov (J.K.G.); jmarcalo@itn.pt (J.M.).
† Oak Ridge National Laboratory.
‡ Instituto Tecnológico e Nuclear.
§ The Ohio State University.
⊥ University of Tennessee.

(1) Edelstein, N. M.; Fuger, J.; Katz, J. J.; Morss, L. R. In *The Chemistry of the Actinide and Transactinide Elements*, 3rd ed.; Morss, L. R., Edelstein, N. M., Fuger, J., Eds.; Springer: Dordrecht, 2006; Vol. 3, pp 1753−1835.
(2) Kaltsoyannis, N.; Hay, P. J.; Li, J.; Blaudeau, J.-P.; Bursten, B. E. In *The Chemistry of the Actinide and Transactinide Elements*, 3rd ed.; Morss, L. R., Edelstein, N. M., Fuger, J., Eds.; Springer: Dordrecht, 2006; Vol. 3, pp 1893−2012.
(3) Denning, R. G. *Struct. Bonding* **1992**, *79*, 215−276.
(4) Fischer, R. D. *Theor. Chim. Acta* **1963**, *1*, 418−431.
(5) Streitweiser, A., Jr.; Müller-Westerhoff, U. *J. Am. Chem. Soc.* **1968**, *90*, 7364−7364.
(6) Streitweiser, A., Jr.; Yoshida, N. *J. Am. Chem. Soc.* **1969**, *91*, 7528−7528.
(7) Karraker, D. G.; Stone, J. A.; Jonew, E. R., Jr.; Edelstein, N. *J. Am. Chem. Soc.* **1970**, *92*, 4841−4845.
(8) Goffart, J.; Fuger, J.; Brown, D.; Duyckaerts, G. *Inorg. Nucl. Chem. Lett.* **1974**, *14*, 15−20.
(9) Brennan, J. G.; Green, J. C.; Redfern, C. M. *J. Am. Chem. Soc.* **1989**, *111*, 2373−2377.
(10) Chang, A. H. H.; Pitzer, R. M. *J. Am. Chem. Soc.* **1989**, *111*, 2500−2507.
(11) Di Bella, S.; Lanza, G.; Fragalá, I. L.; Marks, T. J. *Organometallics* **1996**, *15*, 205−208.
(12) Burns, C. J.; Eisen, M. S. In *The Chemistry of the Actinide and Transactinide Elements*, 3rd ed.; Morss, L. R., Edelstein, N. M., Fuger, J., Eds.; Springer: Dordrecht, 2006; Vol. 5, pp 2799−2910.
(13) Bursten, B. E.; Palmer, E. J.; Sonnenberg, J. L. In *Recent Advances in Actinide Science*; May, I., Alvares, R., Bryan, N., Eds.; Royal Society of Chemistry: Cambridge, UK, 2006; pp 157−162.
(14) Burns, C. J.; Bursten, B. E. *Comments Inorg. Chem.* **1989**, *9*, 61−93.

10.1021/om700329h CCC: $37.00 © 2007 American Chemical Society
Publication on Web 06/30/2007

activation.[15−18] The first study of actinide ion/hydrocarbon reactivity in the gas phase, by Armentrout, Hodges, and Beauchamp, examined the reaction of kinetically excited U^+ ions with CD_4 to produce UD^+.[19,20] Subsequent studies of gas-phase organoactinide ion chemistry have focused on reactions under low-energy conditions, where only inherently thermoneutral or exothermic reactions are observed. The initial low-energy studies employed Fourier transform ion cyclotron resonance mass spectrometry (FTICR/MS) to study reactions of U^+ and Th^+ with hydrocarbons.[21−24] Subsequently, a so-called "laser ablation with prompt reaction and detection" (LAPRD) technique was employed to study reactions of transuranium An^+ ions.[25] These and more recent studies in the field of gas-phase organoactinide ion chemistry have been reviewed.[26,27]

It has been demonstrated that reactivities of gas-phase actinide ions directly reflect their electronic structures and energetics.[26,27] Specifically, the efficiencies of bare An^+ ions (An = Th, Pa, U, Np, Pu, Am, Cm, Bk, Cf, Es) at activating hydrocarbons by an oxidative insertion mechanism were found to inversely correlate with the energies required to excite the ions from their ground states to states with $5f^{n-2}6d7s$ configurations, where *n* represents the total number of electrons of the An^+ ion outside of the closed radon core. Hydrocarbon activation by actinide ions in the gas phase typically proceeds by oxidative insertion into a C−H or C−C bond to form a {C−An^+−H} or {C−An^+−C} type of intermediate. The reduced reactivities of the transuranium ions, Pu^+ through Es^+, are attributed to the requirement for excited-state $5f^{n-2}6d7s$ configurations for such insertions, which indicates that their 5f electrons cannot effectively participate in formation of the two σ-type bonds in the activated intermediate. However, because Th^+, Pa^+, U^+, and Np^+ each have very low-lying ($\Delta E \leq 0.1$ eV) electronic configurations that are inherently reactive, i.e., $5f^{n-2}6d7s$, or $5f^06d^27s$ for Th^+,[28] their higher reactivities do not address the involvement of their 5f electrons in hydrocarbon bond activation. In the present study, quantitative and sensitive measurements of reaction kinetics and product distributions for activation of small alkanes and alkenes by Th^+, Pa^+, U^+, Np^+, Pu^+, Am^+, and Cm^+ are reported. These new results provide a more detailed picture of variations in reactivity across the series and elucidate the role of 5f electrons in organoactinide chemistry.

Addition of an oxo-ligand to a metal ion fundamentally transforms the electronic structure and reactivity of the metal center.[29] As a result, the reactivities of AnO^+ ions provide complementary information to that obtained for the bare An^+ ions. An FTICR/MS study of reactions of ThO^+ and UO^+ with arenes[24] revealed substantially reduced reactivity compared with bare Th^+ and U^+. These results are consistent with the engagement of chemically active valence electrons at the actinide metal centers in the An^+−O bonding. Cornehl et al.[30] similarly found reduced reactivities of CeO^+, NdO^+, ThO^+, and UO^+, as compared with the corresponding bare M^+, toward alkanes and alkenes. However, the latter authors contended that dehydrogenation of 1-butene and 1,4-cyclohexadiene induced by UO^+ provided "... evidence for the participation of 5f electrons in bond formation during activation processes".[30] A special type of reactivity for LnO^+ ions with conjugated dienes (1,3-butadiene and isoprene) has been identified that does not involve an insertion intermediate;[31] however, this type of activation is evidently not generally effective for small alkanes and monoalkenes. Qualitative assessments of comparative reactivities of the AnO^+ for An = Th through Pu, using the LAPRD technique,[26,27] indicated a substantially greater reactivity for PaO^+ as compared with other early AnO^+. However, lacking knowledge about the electronic structure of PaO^+, the significance of this anomalous reactivity could not be conclusively evaluated.[32] In the work reported here, reactions were studied in detail for several small alkanes and alkenes with the AnO^+ ions for An = Th through Cm. In conjunction with these new experimental studies, electronic structure calculations were performed for PaO^+, which now enables an effective evaluation of the distinctive behavior of PaO^+.

Experimental Section

The experimental details have been provided elsewhere,[23,24,33] and only a brief summary is provided here. Ions were produced by laser desorption/ionization of binary actinide/platinum alloys containing ≤20 atom % of natural Th, Pa-231, depleted U, Np-237, Pu-242, Am-243, or Cm-248, using the fundamental 1064 nm wavelength of a Spectra-Physics Quanta-Ray GCR-11 Nd:YAG laser. Desorbed ions directly entered the source cell of a Finnigan FT/MS 2001-DT FTICR/MS equipped with a 3 T magnet and controlled by a Finnigan Venus Odyssey data system. All experiments were carried out in the source cell of the FTICR/MS. Oxide ions were produced directly from the alloys and/or by oxidation of the An^+ ions with pulsed-in O_2 gas. The hydrocarbons were commercial products of >99% purity and were introduced into the spectrometer through a leak valve to pressures of ca. 10^{-8} to 10^{-7} Torr. Pressures were measured with a calibrated[34−37] Bayard-Alpert-type ionization gauge. Isolation of reactant ions was achieved by ejection of other ions using single-frequency, frequency sweep, or

(15) Huang, Y.; Wise, M. B.; Jacobson, D. B.; Freiser, B. S. *Organometallics* **1987**, *6*, 346−354.
(16) Schilling, J. B.; Beauchamp, J. L. *J. Am. Chem. Soc.* **1988**, *110*, 15−24.
(17) Sunderlin, L. S.; Armentrout, P. B. *J. Am. Chem. Soc.* **1989**, *111*, 3845−3855.
(18) Cornehl, H. H.; Heinemann, C.; Schröder, D.; Schwarz, H. *Organometallics* **1995**, *14*, 992−999.
(19) Armentrout, P. B.; Hodges, R.; Beauchamp, J. L. *J. Am. Chem. Soc.* **1977**, *99*, 3162−3163.
(20) Armentrout, P. B.; Hodges, R. V.; Beauchamp, J. L. *J. Chem. Phys.* **1977**, *66*, 4683−4688.
(21) Liang, Z.; Marshall, A. G.; Pires de Matos, A.; Spirlet, J. C. In *Transuranium Elements: A Half Century*; Morss, L. R., Fuger, J., Eds.; American Chemical Society: Washington DC, 1992; pp 247−250.
(22) Heinemann, C.; Cornehl, H. H.; Schwarz, H. *J. Organomet. Chem.* **1995**, *501*, 201−209.
(23) Marçalo, J.; Leal, J. P.; Pires de Matos, A. *Int. J. Mass Spectrom. Ion Processes* **1996**, *157/158*, 265−274.
(24) Marçalo, J.; Leal, J. P.; Pires de Matos, A.; Marshall, A. G. *Organometallics* **1997**, *16*, 4581−488.
(25) Gibson, J. K. *J. Am. Chem. Soc.* **1998**, *120*, 2633−2640.
(26) Gibson, J. K. *Int. J. Mass Spectrom.* **2002**, *214*, 1−21.
(27) Gibson, J. K.; Marçalo, J. *Coord. Chem. Rev.* **2006**, *250*, 776−783.
(28) Blaise, J.; Wyart, J.-F. *Energy Levels and Atomic Spectra of Actinides*; Tables Internationales de Constantes: Paris, 1992.
(29) Schröder, D.; Schwarz, H.; Shaik, S. *Struct. Bonding* **2000**, *97*, 91−123.
(30) Cornehl, H. H.; Wesendrup, R.; Diefenbach, M.; Schwarz, H. *Chem. Eur. J.* **1997**, *3*, 1083−1090.
(31) Cornehl, H. H.; Wesendrup, R.; Harvey, J. N.; Schwarz, H. *J. Chem. Soc., Perkin Trans. 2* **1997**, 2283−2291.
(32) Gibson, J. K.; Haire, R. G. *Inorg. Chem.* **2002**, *41*, 5897−5906.
(33) Santos, M.; Marçalo, J.; Pires de Matos, A.; Gibson, J. K.; Haire, R. G. *J. Phys. Chem. A* **2002**, *106*, 7190−7194.
(34) Bruce, J. E.; Eyler, J. R. *J. Am. Soc. Mass Spectrom.* **1992**, *3*, 727−733.
(35) Lin, Y.; Ridge, D. P.; Munson, B. *Org. Mass Spectrom.* **1991**, *26*, 550−558.
(36) Bartmess, J. E.; Georgiadis, R. M. *Vacuum* **1983**, *33*, 149−153.
(37) Lide, D. R., Ed. *CRC Handbook of Chemistry and Physics*, 75th ed.; CRC Press: Boca Raton, 1994.

Table 1. Products, Rate Constants, and Efficiencies for Reactions of Bare Metal Ions, M^+, with Alkanes and Alkenes[a]

	CH_4	C_2H_6	C_3H_8	*n*-C_4H_{10}	C_2H_4	C_3H_6	1-C_4H_8
Th^+	0.009 [0.10] $ThCH_2^+$ (100)	0.12 [1.1] $ThC_2H_4^+$ (55) $ThC_2H_2^+$ (45)	0.18 [1.8] $ThC_3H_6^+$ (30) $ThC_3H_4^+$ (70)	0.18 [1.8] $ThC_4H_6^+$ (100)	0.34 [3.3] $ThC_2H_2^+$ (100)	0.30 [3.2] $ThC_3H_4^+$ (25) $ThC_3H_2^+$ (20) $ThCH_2^+$ (55)	0.34 [3.5] $ThC_4H_6^+$ (30) $ThC_4H_4^+$ (10) $ThC_2H_2^+$ (40) $ThCH_2^+$ (20)
Pa^+	<0.001	<0.001	0.046 [0.45] $PaC_3H_6^+$ (65) $PaC_3H_4^+$ (35)	0.096 [0.95] $PaC_4H_6^+$ (100)	0.27 [2.6] $PaC_2H_2^+$ (100)	0.25 [2.7] $PaC_3H_4^+$ (65) $PaC_3H_2^+$ (10) $PaCH_2^+$ (25)	0.39 [4.1] $PaC_4H_6^+$ (15) $PaC_4H_4^+$ (75) $PaC_2H_2^+$ (10)
U^+	<0.001	<0.001	0.008 [0.08] $UC_3H_6^+$ (70) $UC_3H_4^+$ (30)	0.078 [0.77] $UC_4H_8^+$ (10) $UC_4H_6^+$ (60) $UC_2H_6^+$ (30)	0.23 [2.3] $UC_2H_2^+$ (100)	0.25 [2.6] $UC_3H_4^+$ (100)	0.29 [3.1] $UC_4H_6^+$ (80) $UC_4H_4^+$ (15) $UC_3H_4^+$ (5)
Np^+	<0.001	<0.001	<0.001	0.010 [0.09] $NpC_4H_8^+$ (20) $NpC_4H_6^+$ (50) $NpC_2H_6^+$ (30)	0.097 [0.94] $NpC_2H_2^+$ (100)	0.28 [3.0] $NpC_3H_4^+$ (100)	0.27 [2.8] $NpC_4H_6^+$ (100)
Pu^+	<0.001	<0.001	<0.001	<0.001	<0.001	<0.001	0.16 [1.6] $PuC_4H_6^+$ (100)
Am^+	<0.001	<0.001	<0.001	<0.001	<0.001	<0.001	<0.001
Cm^+	<0.001	<0.001	<0.001	<0.001	<0.001	0.024 [0.25] $CmC_3H_4^+$ (100)	0.20 [2.1] $CmC_4H_6^+$ (100)
Ta^+	0.070 [0.69] $TaCH_2^+$ (100)	0.31 [3.0] $TaC_2H_4^+$ (20) $TaC_2H_2^+$ (80)	0.28 [2.7] $TaC_3H_4^+$ (100)	0.22 [2.2] $TaC_4H_6^+$ (15) $TaC_4H_4^+$ (85)	0.26 [2.5] $TaC_2H_2^+$ (100)	0.29 [3.1] $TaC_3H_2^+$ (100)	0.34 [3.6] $TaC_4H_4^+$ (80) $TaC_4H_2^+$ (10) $TaC_3H_2^+$ (10)

[a] Reaction efficiencies, k/k_{COL}, are given; pseudo-first-order reaction rate constants, $k/10^{-10}$ cm^3 molecule^{-1} s^{-1}, are in brackets. Absolute values are accurate to ±50%; relative values for comparative purposes are accurate to ±20%. The detection limit of $k/k_{COL} < 0.001$ corresponds to $k < 1 \times 10^{-12}$ cm^3 molecule^{-1} s^{-1}. The product ion distributions are given in parentheses as percentages.

Table 2. Results for Reactions of Metal Monoxide Ions, MO^+, with Alkanes and Alkenes[a]

	C_2H_6	C_3H_8	C_4H_{10}	C_2H_4	C_3H_6	1-C_4H_8
ThO^+	<0.001	<0.001	<0.001	<0.001	<0.001	0.16 [1.7] $ThOC_4H_6^+$ (20) $ThOC_3H_5^+$ (80)
PaO^+	<0.001	0.034 [0.33] $PaOC_3H_6^+$ (80) $PaOC_3H_4^+$ (20)	0.12 [1.2] $PaOC_4H_6^+$ (100)	0.23 [2.2] $PaOC_2H_2^+$ (100)	0.18 [1.9] $PaOC_3H_4^+$ (70) $PaOC_2H_2^+$ (30)	0.43 [4.9] $PaOC_4H_6^+$ (100)
UO^+	<0.001	<0.001	<0.001	<0.001	<0.001	0.01 [0.11] $UOC_4H_6^+$ (100)
TaO^+	0.21 [2.0] $TaOC_2H_4^+$ (100)	0.20 [2.0] $TaOC_3H_4^+$ (100)	0.21 [2.1] $TaOC_4H_6^+$ (80) $TaOC_4H_4^+$ (20)	0.54 [5.3] $TaOC_2H_2^+$ (100)	0.17 [1.8] $TaOC_3H_4^+$ (100)	0.36 [3.8] $TaOC_4H_4^+$ (100)
NpO^+	<0.001	<0.001	<0.001	<0.001	<0.001	<0.001
PuO^+	<0.001	<0.001	<0.001	<0.001	<0.001	<0.001
AmO^+	<0.001	<0.001	<0.001	<0.001	<0.001	<0.001
CmO^+	<0.001	<0.001	<0.001	<0.001	<0.001	<0.001

[a] The results are reported as described in Table 1. As indicated, the four studied transuranic AnO^+ were unreactive with the alkanes and alkenes. All eight studied MO^+ were unreactive with CH_4 to within the detection limit: $k/k_{COL} < 0.001$; $k < 1 \times 10^{-12}$ cm^3 molecule^{-1} s^{-1}.

SWIFT excitation.[38] Reactant ions were cooled by collisions with argon, and their thermalization was confirmed by reproducibility of reaction kinetics and product distributions, as well as by linearity of the pseudo-first-order reactant ion decay plots. Pseudo-first-order reaction rate constants, k, were determined from the decay of the reactant ion signals as a function of time at constant neutral reagent pressures. Reaction efficiencies are reported as k/k_{COL}, where k_{COL} is the collisional rate constant derived from the modified variational transition-state/classical trajectory theory of Su and Chesnavich.[39] Uncertainties of ±50% are assigned to the absolute rate constants; relative uncertainties in the reported rate constants, k and k/k_{COL}, are estimated as ±20%.

Results and Discussion

FTICR/MS Experiments. Gas-phase reactivities were examined for monopositive actinide and actinide monoxide ions, An^+ and AnO^+, where An = Th, Pa, U, Np, Pu, Am, or Cm. In addition, Ta^+ and TaO^+ were studied for comparative purposes, particularly with Pa, which could present a behavior typical of a group 5, d-block transition metal. The neutral reaction partners were methane, ethane, propane, *n*-butane, ethene, propene, and 1-butene. For Pa^+, PaO^+, Ta^+, and TaO^+ the reactions with 1,3-butadiene and isoprene were also examined for comparison with results reported previously for other M^+ and MO^+ ions.[31,40] The reactivity results for the bare and oxo-ligated metal ions are summarized in Tables 1−3. The results are reported as reaction efficiencies, k/k_{COL}, with the corresponding pseudo-first-order reaction rate constants, k, given in brackets, and the product distributions with their percent contributions given in parentheses. As the primary reactions were most informative, secondary and higher-order reactions were not studied.

As is evident from data in Table 1, there was a wide variation in both the reaction rates/efficiencies and product distributions for the eight bare metal ions. Only Am^+ was found to be inert

(38) Guan, S.; Marshall, A. G. *Int. J. Mass Spectrom. Ion Processes* **1996**, *157/158*, 5−37.
(39) Su, T.; Chesnavich, W. J. *J. Chem. Phys.* **1982**, *76*, 5183−5185.
(40) Santos, M.; Marçalo, J.; Leal, J. P.; Pires de Matos, A.; Gibson, J. K.; Haire, R. G. *Int. J. Mass Spectrom.* **2003**, *228*, 457−465.

Table 3. Results for Reactions of Pa^+, PaO^+, Ta^+, and TaO^+ with 1,3-Butadiene and Isoprene[a]

	C_4H_6	C_5H_8
Pa^+	0.61 [6.4]	0.66 [7.0]
	$PaC_4H_4^+$ (20)	$PaC_5H_6^+$ (5)
	$PaC_4H_2^+$ (15)	$PaC_5H_4^+$ (40)
	$PaC_3H_3^+$ (15)	$PaC_3H_4^+$ (45)
	$PaC_2H_2^+$ (50)	$PaC_2H_2^+$ (10)
PaO^+	0.47 [4.9]	0.67 [7.0]
	$PaOC_4H_4^+$ (20)	$PaOC_5H_8^+$ (5)
	$PaOC_2H_2^+$ (80)	$PaOC_5H_6^+$ (5)
		$PaOC_5H_5^+$ (5)
		$PaOC_3H_4^+$ (60)
		$PaOC_2H_2^+$ (25)
Ta^+	0.60 [6.4]	0.66 [7.1]
	$TaC_4H_4^+$ (5)	$TaC_5H_4^+$ (40)
	$TaC_4H_2^+$ (60)	$TaC_4H_2^+$ (10)
	$TaC_3H_3^+$ (5)	$TaC_3H_4^+$ (25)
	$TaC_2H_2^+$ (30)	$TaC_3H_2^+$ (15)
		$TaC_2H_2^+$ (10)
TaO^+	0.56 [5.9]	0.69 [7.3]
	$TaOC_4H_4^+$ (25)	$TaOC_5H_4^+$ (75)
	$TaOC_4H_2^+$ (65)	$TaOC_4H_2^+$ (10)
	$TaOC_2H_2^+$ (10)	$TaOC_3H_4^+$ (15)

[a] The results are reported as described in Table 1.

toward all seven hydrocarbons, to within the detection limit. The present results are in accord with previous FTICR/MS studies of corresponding reactions of Th^+[23] and U^+[22] ions. Rate constants reported by Heinemann et al.[22] for the same U^+/hydrocarbon reactions were consistently higher, by a factor of 2−4, than the corresponding values reported here; these discrepancies presumably reflect uncertainties associated with the absolute rate constants. The relative uncertainties of the rates obtained in the present study are substantially smaller than the absolute uncertainties and show, in the case of U^+, the same trend as obtained by Heinemann et al.[22] The reactivity patterns for Ta^+ in the present work are also in accord with previous results,[41] except that for the Ta^+/C_3H_8 reaction the reported 22% $TaC_3H_2^+$ channel corresponding to triple H_2-elimination[41] was not observed here. Some products previously reported for Pa^+ from LAPRD experiments[32] were also not observed in the present work. Particularly noteworthy was the absence of PaC_2^+ from the Pa^+/C_3H_6 reaction, and PaC_4^+ from the Pa^+/C_4H_8 reaction. The intriguing protactinium dicarbide and tetracarbide ions reported previously as minor products[32] are evidently not produced under low-pressure, thermal FTICR/MS conditions, suggesting new reaction channels under LAPRD conditions.

Reactions that resulted in metal carbene ions are summarized by eqs 1−3, where the lower limits for the metal ion−carbene bond strengths required for thermoneutral/exothermic reactions are as indicated.[42]

$$M^+ + CH_4 \rightarrow MCH_2^+ + H_2 \qquad D[M^+-CH_2] \geq 465 \text{ kJ mol}^{-1} \quad M = \text{Th, Ta} \quad (1)$$

$$M^+ + C_3H_6 \rightarrow MCH_2^+ + C_2H_4 \qquad D[M^+-CH_2] \geq 422 \text{ kJ mol}^{-1} \quad M = \text{Th, Pa} \quad (2)$$

$$M^+ + C_4H_8 \rightarrow MCH_2^+ + C_3H_6 \qquad D[M^+-CH_2] \geq 411 \text{ kJ mol}^{-1} \quad M = \text{Th} \quad (3)$$

As discussed below, the initial product for these dehydrogenation processes is presumably an oxidative insertion intermediate (e.g., $\{H-M^+-CH_3\}$ for methane), which spontaneously eliminates H_2 or a hydrocarbon. Although Pa^+ did not activate methane, the protactinium carbene ion was produced according to eq 2. The thorium carbene ion was produced according to eqs 1, 2, and 3, while the Ta^+ carbene resulted only from eq 1. The implications that $D[Ta^+-CH_2] \geq 465$ kJ mol^{-1} from eq 1 and $D[Pa^+-CH_2] \geq 422$ kJ mol^{-1} from eq 2 indicate that eq 3 is exothermic for Ta^+ and Pa^+. The $D[Pa^+-CH_2]$ bond strength, ≥ 422 kJ mol^{-1}, is greater than first- and second-row transition metal ion−carbene bond strengths, with the possible exceptions of $D[Zr^+-CH_2]$ and $D[Nb^+-CH_2]$, and is apparently comparable to $D[M^+-CH_2]$ for the third-row transition metals.[43] Together with eqs 2 and 3, other reactions that result in carbon−carbon bond cleavage are given by eqs 4−6.

$$M^+ + C_4H_{10} \rightarrow MC_2H_6^+ + C_2H_4 \quad M = \text{U, Np} \quad (4)$$

$$M^+ + C_4H_8 \rightarrow MC_3H_4^+ + CH_4 \quad M = \text{U} \quad (5)$$

$$M^+ + C_4H_8 \rightarrow MC_3H_2^+ + CH_4 + H_2 \quad M = \text{Ta} \quad (6)$$

Heinemann et al.[22] performed collision-induced dissociation (CID) studies of the $UC_2H_6^+$ product of eq 4, which suggested the dimethyl structure, $U(CH_3)_2^+$.

Other than the reactions given by eqs 2−6, the reactions reported in Table 1 correspond to carbon−hydrogen activation(s) and loss of one, two, or three hydrogen molecules. Single and multiple hydrogen eliminations are also typically the dominant pathways for reactions of Ln^+ with small alkanes and alkenes under low-energy conditions[15−18] and are characteristic of oxidative insertion mechanisms.

The results in Table 2 for the reactions of ThO^+ and UO^+ are in good agreement with those reported by Cornehl et al.[30] For the same seven hydrocarbons, inert behavior was also observed in the previous study, except with 1-butene, for which reaction efficiencies of 0.22 for ThO^+ (versus 0.16 here) and 0.008 for UO^+ (versus 0.01 here) were reported;[30] their product distributions[30] were the same as in Table 2. TaO^+ was previously found to be inert toward methane[44] and active toward 1-butene,[45] although, in this last case, somewhat different product distributions were observed, probably due to different experimental conditions. Reactions of PaO^+ with propene and 1-butene were also studied previously by LAPRD.[32] In qualitative accord with the present results, the main product from the PaO^+/C_3H_6 reaction was $PaOC_3H_4^+$ and that from $PaO^+/1\text{-}C_4H_8$ was $PaOC_4H_6^+$.[32] As noted above, some minor products appeared under the higher pressure, potentially hyperthermal conditions of LAPRD experiments that were not observed for the lower pressure, thermal FTICR/MS experiments. For example, the present results demonstrated that CmO^+ is inert toward all studied hydrocarbons, whereas it was previously reported from

(41) Buckner, S. W.; MacMahon, T. J.; Byrd, G. D.; Freiser, B. S. *Inorg. Chem.* **1989**, *28*, 3511−3518.
(42) Lias, S. G.; Bartmess, J. E.; Liebman, J. F.; Holmes, J. L.; Levin, R. D.; Mallard, W. G. *J. Phys. Chem. Ref. Data* **1988**, *17* (Suppl. 1).
(43) Armentrout, P. B. In *The Encyclopedia of Mass Spectrometry*; Gross, M. L., Caprioli, R., Eds.; Elsevier: Amsterdam, 2006; Vol. 1, pp 800−810.
(44) Wesendrup, R.; Schwarz, H. *Angew. Chem., Int. Ed. Engl.* **1995**, *34*, 2033−2035.
(45) Zemski, K. A.; Bell, R. C.; Castleman, A. W., Jr. *Int. J. Mass Spectrom.* **1999**, *184*, 119−128.

Table 4. Energies of Low-lying $5f^{n-1}$, $5f^{n-2}$, and $5f^{n-3}$ Configurations of An^+ Ions[a]

	$5f^{n-1}7s$	$5f^{n-1}6d$	$5f^{n-2}7s^2$	$5f^{n-2}6d7s$	$5f^{n-2}6d^2$	$5f^{n-3}6d^27s$
Th^+ ($n = 3$)	3.02	4.04	0.56	0.76	1.55	0/ground
Pa^+ ($n = 4$)	0.99 ± 0.12	2.0 ± 0.4	0/ground	0.10	0.92	0.59
U^+ ($n = 5$)	0.58	1.55	0/ground	0.04	0.57	1.71
Np^+ ($n = 6$)	0.01	1.17	0.003	0/ground	0.9 ± 0.4	~2.7
Pu^+ ($n = 7$)	0/ground	1.49	1.02	1.08	2.14	4.67
Am^+ ($n = 8$)	0/ground	1.7 ± 0.1	2.3 ± 0.1	2.5 ± 0.1	3.6 ± 0.2	7.3 ± 0.6
Cm^+ ($n = 9$)	0.26	2.13	0/ground	0.50	1.84	6.7 ± 0.4

[a] Energies of the lowest lying term for the indicated configuration from ref 28 in eV (1 eV = 96.49 kJ mol^{-1}). Each configuration additionally includes the inner radon core electrons.

LAPRD that the $CmO^+/1\text{-}C_4H_8$ reaction resulted in small amounts of $CmOC_4H_6^+$ and $CmOC_4H_8^+$.[46]

The results for reactions of bare Pa^+ and Ta^+ with 1,3-butadiene (C_4H_6) and isoprene (C_5H_8) in Table 3 can be compared with previous results for Th^+, U^+, Np^+, Pu^+, and Am^+ with these dienes.[40] Whereas Pu^+ and Am^+ were inert toward C_4H_6, the Th^+, U^+, and Np^+ ions reacted efficiently to give $MC_2H_2^+$ as the dominant product;[40] the reactivities of Pa^+ and Ta^+ are similar to these latter three ions except that $TaC_4H_2^+$ was more abundant than $TaC_2H_2^+$. Six of the seven M^+ studied previously[40] or in the present work reacted with isoprene; only Am^+ was inert. For five of the six reactive metal ions, the most abundant product with C_5H_8 was $MC_3H_4^+$ ($PuC_3H_4^+$ and $PuC_5H_6^+$ were equally abundant[40]); among the metal ions studied, Ta^+ was again distinctive, with $TaC_5H_4^+$ being the most abundant product. The variations in the reaction rate constants and product distributions for reactions of the bare metal ions with dienes are consistent with the ions' comparative reactivities with alkanes and alkenes (discussed below). The reactivities reported in Table 3 for PaO^+ and TaO^+, in comparison with reactions of other MO^+ ions with these dienes, are also discussed below.

Comparative Reactivities of Bare Metal Ions. The energies of pertinent electronic configurations of free actinide ions, An^+, are given in Table 4.[28] For each An^+ with a total of n electrons outside of its closed radon core, the low-lying states with one, two, and three non-5f electrons are included in Table 4 (i.e., $5f^{n-1}$, $5f^{n-2}$, and $5f^{n-3}$). In each case, the lowest energy $5f^{n-x}$ configuration with a 7p valence electron is significantly higher in energy than the specified $5f^{n-x}$ configurations. The $5f^{n-3}6d^27s$ are the lowest lying $5f^{n-3}$ configurations; for Cm^+ the $5f^{n-3}6d^27s$ (at 6.7 ± 0.4 eV) and $5f^{n-3}6d7s^2$ (at 6.7 ± 0.3 eV) configurations are essentially degenerate.[28] The energy of the lowest term of each configuration is given. All of the configurations are high-spin, i.e., $S = \{2n + 1\}$, except for $S = \{2(n - 2) + 1\}$ for all of the $7s^2$ configurations, as well as for the $5f^8$ configurations of Cm^+. The ground state of Ta^+ is high-spin ^5F, $5d^36s$.[47]

An important result reported previously[23] and reproduced here is the dehydrogenation of methane by Th^+ (eq 1). Methane dehydrogenation to produce MCH_2^+ is exothermic for several 5d-transition metal ions (Ta^+, W^+, Os^+, Ir^+, and Pt^+).[41,48−51] As the reactivity of d-block transition metal ions in general increases down a given group, it is an apparent anomaly that Hf^+ does not activate CH_4,[50−52] whereas the reaction of Zr^+ is only slightly endothermic.[53,54] The reduced reactivity of Hf^+ has been attributed to its ^2D, $5d6s^2$ ground-state electronic configuration,[52] which, in contrast to the Zr^+ ground state, ^4F, $4d^25s$, lacks two spin-unpaired valence electrons for insertion into a C−H bond. The only An^+ ion known to exothermically dehydrogenate methane[23] is Th^+, which has a ^4F, $6d^27s$ ground electronic state[28] and accordingly exhibits reactivity that is characteristic of a d-block transition metal ion. It is notable that a recent theoretical study[55] indicated that the 5f orbitals play an important role in the activation of methane by neutral Th atoms. The Rf^+/CH_4 reaction would be of interest to evaluate the electronic structure of this first transactinide ion. The ground state of Rf^+ has been calculated as ^2D, $5f^{14}6d7s^2$, with no low-lying quartet configurations.[56] In analogy with ^2D Hf^+, it would be expected that ^2D Rf^+ is inert toward methane activation. If, as reported,[56] all of its excited states up to ~4 eV are ^2D ($5f^{14}6d7s^2$) or ^2P ($5f^{14}7s^27p$), then Rf^+ should be substantially more inert toward activation of larger hydrocarbons than is Hf^+, as the reactive ^4F ($5d^26s$) configuration of Hf^+ lies only 0.56 eV above ground.[52]

The reactivity patterns reported for the bare metal ions in Table 1—primarily single and multiple H_2-elimination—are typical of an oxidative insertion mechanism with a {C−M^+−H} type of intermediate in which the metal center has formed two σ-type bonds. This mechanism has been commonly used to explain dehydrogenation (and other small-molecule eliminations) from C_1 to C_4 hydrocarbons by thermal, open-shell, d- and f-block metal ions. (In the particular case of closed-shell (d^{10}) Au^+ ions, another mechanism has been recently unveiled.[57])

The previous ordering of reactivities, derived primarily from LAPRD results, was as follows:[26,27]

$$Th^+ \geq Pa^+ \geq U^+ \approx Np^+ > Cm^+ \geq Pu^+ > Am^+$$

The results obtained in the present work using the more sensitive and quantitative FTICR/MS technique, and additional hydrocarbons, have elaborated and refined these comparative reactivities. The results for alkanes (Table 1) clearly reveal that the reactivity decreases as $Th^+ > Pa^+ > U^+ > Np^+$. Also, the results for propene show that Cm^+ is more reactive than Pu^+. The particularly low reactivity of Am^+ was confirmed. The

(46) Gibson, J. K.; Haire, R. G. *J. Phys. Chem. A* **1998**, *102*, 10746−10753.
(47) Moore, C. E. *Atomic Energy Levels, Vol. 3*; National Bureau of Standards (NIST): Washington, DC, 1958.
(48) Irikura, K. K.; Beauchamp, J. L. *J. Am. Chem. Soc.* **1989**, *111*, 75−85.
(49) Irikura, K. K.; Beauchamp, J. L. *J. Am. Chem. Soc.* **1991**, *113*, 2769−2770.
(50) Irikura, K. K.; Beauchamp, J. L. *J. Phys. Chem.* **1991**, *95*, 8344−8351.
(51) Irikura, K. K.; Goddard, W. A. *J. Am. Chem. Soc.* **1994**, *116*, 8733−8740.
(52) Parke, L. G.; Hinton, C. S.; Armentrout, P. B. *Int. J. Mass Spectrom.* **2006**, *254*, 168−182.
(53) Ranasinghe, Y. A.; MacMahon, T. J.; Freiser, B. S. *J. Phys. Chem.* **1991**, *95*, 7721−7726.
(54) Armentrout, P. B.; Sievers, M. R. *J. Phys. Chem. A* **2003**, *107*, 4396−4406.
(55) de Almeida, K. J.; Cesar, A. *Organometallics* **2006**, *25*, 3407−3416.
(56) Eliav, E.; Kaldor, U.; Ishikawa, Y. *Phys. Rev. Lett.* **1995**, *74*, 1079−1082.
(57) Li, F.-X.; Armentrout, P. B. *J. Chem. Phys.* **2006**, *125*, 133114.

refined ordering of reactivities from the present FTICR/MS results (Table 1) is

$$Th^+ > Pa^+ > U^+ > Np^+ > Cm^+ > Pu^+ > Am^+$$

As the valence state of the metal center in the oxidative insertion intermediate (e.g., {C−M$^+$−H}) is formally +3, the reactivity of a given metal ion might be thought to correlate with the ease of the "oxidation" (gas phase) process given by eq 7.

$$M^+ \rightarrow M^{3+} + 2e^- \quad (7)$$

The energy for eq 7 is the sum of the second and third ionization energies: ΔE[eq 7] = IE[M$^+$] + IE[M^{2+}] ≡ IE$_{2,3}$[M]. Bratsch and Lagowski[58] have provided the following estimates for IE$_{2,3}$[An] (in eV):

$$Pa\ (31.2) < Th\ (31.5) \approx U\ (31.5) < Np\ (32.1) < Pu\ (33.2) < Cm\ (33.3) < Am\ (34.0)$$

It may appear that there is some correlation between these IE$_{2,3}$[An] and the comparative reactivities observed for the An$^+$ ions; however, the correlation is not rigorously established. In previous LAPRD results for Bk$^+$[59] it was indicated that Bk$^+$ is more effective than Am$^+$ at oxidative insertion;[26,27] this is the opposite trend predicted from IE$_{2,3}$[Bk] = 34.3 eV.[58] Further, results from Cornehl et al.[18] for Ln$^+$ ion reactivities also indicate that eq 7 is not directly germane to gas-phase oxidative insertion reactions. For example, it was found there[18] that Lu$^+$ is much more reactive than Sm$^+$, although IE$_{2,3}$[Lu] = 34.9 eV is greater than IE$_{2,3}$[Sm] = 34.5 eV.[60] Instead, Cornehl et al.[18] identified promotion to a reactive divalent state of the metal ion as the factor that determines the ease of oxidative insertion. This latter model is consistent with covalent metal−hydrogen and/or metal−carbon bond formation in the "oxidative insertion" intermediates. Finally, the magnitude of IE$_{2,3}$[M] (>30 eV) compared with the ionization energies of the "ligands" in the oxidative insertion intermediate, e.g., IE[H] = 13.6 eV and IE[CH$_3$] = 9.8 eV,[42] establishes that a direct role of M^{3+} ions in these gas-phase organometallic complexes is implausible. Instead, we adopt the promotion energy concept discussed below.

The reactive electronic state for oxidative insertion by An$^+$ ions is 5f^{n-2}6d7s (or the ground state 5f^{0}6d^{2}7s for Th$^+$), if the 5f electrons cannot effectively participate in bond activation.[26,27] The promotion energies from the ground state to these non-5f divalent reactive states are given in Table 4 and exhibit the following ordering (with the energies in eV[28]):

$$Th^+\ (0) \approx Pa^+\ (0.10) \approx U^+\ (0.04) \approx Np^+\ (0) < Cm^+\ (0.50) < Pu^+\ (1.08) < Am^+\ (\sim 2.5)$$

The promotion energies for the first four are within 0.10 eV of the ground state, which is too small a variation to have a significant effect on oxidative insertion efficiencies.[18,52] The decrease in reactivity beyond Np$^+$ is as would be predicted if the 5f electrons are chemically inert, and promotion to the lowest lying 5f^{n-2}6d7s configuration is necessary for effective oxidative insertion.

It is apparent that the comparative reactivities of Th$^+$, Pa$^+$, U$^+$, and Np$^+$ are not explicable from their very small promotion energies. To the extent that the small difference between these energies might be manifested in reaction efficiencies, the following ordering would have been predicted: Th$^+$ ≈ Np$^+$ > U$^+$ > Pa$^+$. The distinctively high reactivity of Th$^+$ is tentatively attributed to its quartet 6d^{2}7s ground-state configuration.[23,52,54] The comparative reactivities of Pa$^+$, U$^+$, and Np$^+$ are intriguing, as the ordering is opposite of what would be predicted from the very small differences in promotion energies.

A consequence of oxidative insertion of a metal ion into a C−H or C−C bond via formation of two covalent bonds is a loss of electron exchange energy, K, associated with the two valence electrons at the metal center, which are spin-unpaired prior to their involvement in bond formation.[61] This issue has been addressed for the lanthanide ions, Ln$^+$, for which the loss of exchange energy, ΔK, from the 4f^{n-2}5d6s prepared divalent state is given by eq 8.[18]

$$\Delta K = K_{d-s} + u_f\{1/2(K_{d-f} + K_{s-f})\} \quad (8)$$

For the lanthanides, K_{d-s} is the 5d−6s exchange energy, which can be assumed to be nearly constant.[18] The quantity $1/2(K_{d-f} + K_{s-f})$ represents the average 5d−4f and 6s−4f exchange energy per unpaired 4f electron; u_f is the number of unpaired 4f electrons, which is $n - 2$ for the early Ln$^+$ through Gd$^+$. Assuming that $(K_{d-f} + K_{s-f})$ is constant, differences in ΔK are due to variations in u_f. Cornehl et al.[18] estimated $1/2(K_{d-f} + K_{s-f})$ as ∼30 kJ mol^{-1} for the Ln$^+$, but a subsequent evaluation[62] suggested a value of only ∼10 kJ mol^{-1} for K_{d-f}. The results of a theoretical treatment[63] also indicated that the 5d−4f exchange energy in lanthanide atoms is minor. As the overlap of the radial distribution functions for 6s/4f orbitals is less than that for 5d/4f,[64] K_{s-f} should be smaller than K_{d-f}. The observed reactivities of the Ln$^+$ ions toward hydrocarbons are in accord with a minor influence of 5d−4f and 6d−4f exchange energies. For example, $u_f = 0$ for La$^+$(4f^{0}5d6s) and $u_f = 7$ for Gd$^+$(4f^{7}5d6s), but both ions exhibit a similar high reactivity toward alkanes.[18] The additional loss of exchange energy, $7 \times \{1/2(K_{d-f} + K_{s-f})\}$, for the Gd$^+$ ion evidently does not appreciably diminish its reactivity.

The influence of exchange energy can similarly be assessed for An$^+$ ions. Applying eq 8 to the An$^+$, K_{d-s} is the 6d−7s exchange energy and $1/2(K_{d-f} + K_{s-f})$ is the average 6d−5f and 7s−5f exchange energy per unpaired 5f electron, u_f. The efficiency of oxidative insertion of An$^+$ ions might decrease with increasing loss of exchange energy from the 5f^{n-2}6d7s configuration suitable for oxidative insertion.[26,27] The 6d−7s exchange energy, K_{d-s}, should be nearly constant, and the second term in eq 8 should increase as u_f. The loss of 5f−6d and 5f−7s exchange energies, ΔK, should thus increase in the order Pa$^+$(^{5}K, 5f^{2}6d7s; u_f =2) < U$^+$(^{6}L, 5f^{3}6d7s; u_f = 3) < Np$^+$(^{7}L, 5f^{4}6d7s; u_f = 4),[28] which may decrease the efficiency of hydrocarbon activation from Pa$^+$ to Np$^+$. An analysis of bonding in actinide monoxides[62] suggested that the 6d−5f exchange energy is minor: $K_{d-f} \leq 10$ kJ mol^{-1}; as the radial distribution function overlap for 7s/5f orbitals is less than for 6d/5f,[64] it is expected that $K_{s-f} < K_{d-f}$. This assessment implies that loss of 6d−5f and 7s−5f exchange energies should have a

(58) Bratsch, S. G.; Lagowski, J. J. *J. Phys. Chem.* **1986**, *90*, 307−312.
(59) Gibson, J. K.; Haire, R. G. *Radiochim. Acta* **2001**, *89*, 709−719.
(60) Johnson, D. A. *Some Thermodynamic Aspects of Inorganic Chemistry*, 2nd ed.; Cambridge University Press: Cambridge, 1982.
(61) Carter, E. A.; Goddard, W. A. *J. Phys. Chem.* **1988**, *92*, 5679−5683.
(62) Gibson, J. K. *J. Phys. Chem. A* **2003**, *107*, 7891−7899.
(63) Sekiya, M.; Narita, K.; Tatewaki, H. *Phys. Rev. A* **2001**, *63*, 012503.
(64) Seijo, L.; Barandiarán, Z.; Harguindey, E. *J. Chem. Phys.* **2001**, *114*, 118.

negligible effect on oxidative insertion efficiencies of the An^+ ions; the comparative reactivities of the An^+ ions support this. For example, the significantly higher reactivity of Cm^+ compared with Pu^+ is well explained by the difference between the promotion energies (Table 4) to the ^{10}D Cm^+ ($5f^7 6d7s$; $\Delta E = 0.50$ eV) and ^8K Pu^+ ($5f^5 6d7s$; $\Delta E = 1.08$ eV) excited states. The greater $u_f\{1/2(K_{d-f} + K_{s-f})\}$ for ^{10}D Cm^+ ($u_f = 7$) versus ^8K Pu^+ ($u_f = 5$) is evidently insignificant relative to the 0.58 eV (56 kJ mol^{-1}) difference in excitation energies.

The differences in exchange energy losses for oxidative insertion, i.e., $\Delta K[Np^+] > \Delta K[U^+] > \Delta K[Pa^+]$, should not result in significant differences in reactivity, and therefore, it is proposed that the differences in reactivities of Pa^+, U^+, and Np^+ reflect differing participation of 5f electrons in C−H bond activation: Pa^+ ($5f^2 6d7s$) > U^+ ($5f^3 6d7s$) > Np^+ ($5f^4 6d7s$). The quartet $6d^2 7s$ ground-state configuration of Th^+ is more reactive than the triplet 6d7s configuration, and this may be due to the availability of an additional 6d electron for participation in bond activation. In analogy with the apparent effect of an additional 6d electron on the reactivity of Th^+, participation of one or more 5f valence electrons in activation should enhance the efficacy of An^+ insertion. It is for the early actinides that the greatest degree of covalency involving 5f orbitals is expected.[14] The interpretation of the present results is in accord with this: the greatest 5f participation for Pa^+, less 5f participation for U^+, and no discernible 5f participation for Np^+. The results for AnO^+ reactivities discussed below are also in accord with the postulated maximum 5f participation in organoactinide σ-type bonding for Pa.

Electronic Structure Calculations for PaO^+. Interpretation of the reactivity results for the metal oxide ions requires knowledge of their electronic structures. As is readily apparent from the results in Table 2 and discussed in detail below, the reactivity of PaO^+ is distinctive among the studied AnO^+. To effectively interpret these results, electronic structure calculations were performed for PaO^+. Spin−orbit configuration interaction calculations with single and double electron excitations (SO-CISD)[65] were performed to determine the electronic ground state, equilibrium bond length, and the low-lying excited states of PaO^+. The SOCISD calculations utilize relativistic effective core potentials (RECPs) containing a medium size core (68 electrons) for the protactinium atom and a RECP for the two electrons in the 1s orbital of the oxygen atom.[65−67] RECP implementation suggests use of RECP basis sets[68,69] approximating the correlation consistent polarized valence double-ζ (cc-pVDZ) level, (6s6p6d4f1g)/[4s3p3d2f1g] on the actinide atom and a (4s4p1d)/[3s2p1d] on the oxygen.

To accommodate the large number of electrons (98 electrons in PaO^+) and importance of relativity, including spin−orbit coupling, within these molecules, the electrons are incorporated as one of three types to make the calculations feasible. The first type consists of the core electrons in the RECPs, which correspond to the 70 inner most core electrons: two electrons from the oxygen 1s electrons and the remaining 68 Pa electrons filling the 1s to 5p shells. The RECP does not include the 5d electrons, the 6s/6p electrons on the Pa, and the 2s electrons of oxygen, which are incorporated into the calculation as the second type: uncorrelated frozen-core electrons consisting of mainly atomic shells. The third type are the outermost eight electrons, which are correlated in an active space that includes molecular orbitals 5σ, 3π, 1φ, 2δ, 6σ, 3δ, 4π, 7σ, 5π, and 8σ that correspond to mixes of atomic orbitals from the 5f/6d/7s/7p on Pa and the 2p shell on oxygen. The O atom splits the 6d orbitals more than the 5f orbitals so that the only 6d orbital to play a major role in these states is $6d_\delta$. SOCISD is carried out with this reference space and all single and double excitations out of it, resulting in determination of bond length and excitation energies with $\sim 4.6 \times 10^6$ spin eigenfunctions.

Table 5. Calculated Orbital Occupations and Contributing Terms for Low-Lying Electronic States of PaO^+[a]

ΔE (eV)	orbital occupation	contributing term(s) (%)
0.000	$5f^{1.0}6d^{1.0}$	86.6 $^3H_4$
0.174	$5f^{1.0}7s^{1.0}$	78.4 $^3\Phi_2$
0.235	$5f^{1.0}7s^{1.0}$	47.7 $^3\Phi_3$ 29.8 $^1\Phi_3$ [b]
0.494	$5f^{1.0}6d^{1.0}$	88.3 $^3H_5$
0.724	$5f^{1.0}7s^{1.0}$	85.9 $^3\Phi_4$
0.981	$5f^{1.0}6d^{1.0}$	92.4 $^3H_6$

[a] Only states up to 1 eV with near-integer atomic-like orbital occupations are included here. All 63 identified electronic states from 0 to 1.8 eV, with near-integer and non-integer occupations, are provided as Supporting Information. The lowest lying 5f-depleted state—$5f^n$ with $n < 1$—is $5f^{0.8}6d^{0.5}7s^{0.7}\Delta_1$ at 0.373 eV. All states up to 1.8 eV have a $5f^n$ occupation of $n \geq 0.8$ (see Figure 1 and the Supporting Information). [b] The substantial mixing of $^3\Phi_3$ and $^1\Phi_3$ suggests intermediate coupling for this state.

For PaO^+, an SCF calculation was completed, indicating a ground state of $^3H_4$, with the two unpaired electrons occupying the $5f_\varphi$ and $6d_\delta$ orbitals. Excited states have 5f, 6d, and 7s orbitals (i.e., $f_\varphi s$, $d_\delta f_\pi$, $f_\varphi f_\pi$) occupied. Improvement of the SCF virtual molecular orbitals (MOs) for excited-state wave functions was completed by means of the improved virtual orbital (IVO) transformation.[70] The IVO calculation gives a single set of MOs that represent the best description of both the ground state and the low-lying excited states. Using the optimized MO coefficients for the ground state $^3H_4$, the intermolecular distance was varied and the equilibrium bond length was found to be 1.852 Å. Whereas the bond length for PaO^+ might be expected to be similar to those for ThO^+ and UO^+, this calculated value for PaO^+ is actually somewhat longer than the experimental values of 1.807 Å for ThO^+ and 1.801 Å for UO^+.[71]

Some of the results of the calculations for PaO^+ are given in Table 5, expressed as the configuration energies relative to the ground state, the orbital occupations, and the contributing terms. Only the ground state ($\Delta E = 0$) and the five lowest lying ($\Delta E \leq 1$ eV) excited states with near-integer orbital occupations (i.e., $5f^{1.0}6d^{1.0}7s^{0.0}$ or $5f^{1.0}6d^{0.0}7s^{1.0}$) are given in Table 5; all of the 62 excited states up to 1.8 eV are provided in the Supporting Information. The 7p orbitals were also considered in the calculations but were unoccupied for all states, i.e., $7p^{0.0}$. The results of the calculations are summarized in Figure 1, where the orbital occupations of all states up to 1.8 eV are plotted as a function of excitation energy. The calculated orbital occupancies—tabulated and plotted—have been rounded to the nearest 0.1 electron to reflect the estimated uncertainties.

Goncharov and Heaven[72] used the pulsed field ionization−zero kinetic-energy photoelectron spectroscopy (PFI-ZEKE) technique to demonstrate that the ground electronic state of ThO^+ originates from $Th^{3+}(7s)O^{2-}$ and the low-lying excited

(65) Lischka, H.; Shepard, R.; Pitzer, R. M.; Shavitt, I.; Dallos, M.; Müller, T.; Szalay, P. G.; Seth, M.; Kedziora, G. S.; Yabushita, S.; Zhang, Z. *Phys. Chem. Chem. Phys.* **2001**, *3*, 664−673.

(66) Christansen, P. A. Unpublished, Oct. 29, 1999. Available at www.chemistry.ohio-state.edu/~pitzer/docs/arep/pa68 and www.chemistry.ohio-state.edu/~pitzer/docs/hso/pa68.

(67) Pacios, L. F.; Christiansen, P. A. *J. Chem. Phys.* **1985**, *82*, 2664−2671.

(68) Blaudeau, J.-P.; Brozell, S. R.; Matsika, S.; Zhang, Z.; Pitzer, R. M. *Int. J. Quantum Chem.* **2000**, *77*, 516−520.

(69) Christiansen, P. A. *J. Chem. Phys.* **2000**, *112*, 10070−10074.

(70) Hunt, W. S.; Goddard, W. A. *Chem. Phys. Lett.* **1969**, *3*, 414−418.

(71) Heaven, M. C. *Phys. Chem. Chem. Phys.* **2006**, *8*, 4497−4509.

(72) Goncharov, V.; Heaven, M. C. *J. Chem. Phys.* **2006**, *124*, 064312.

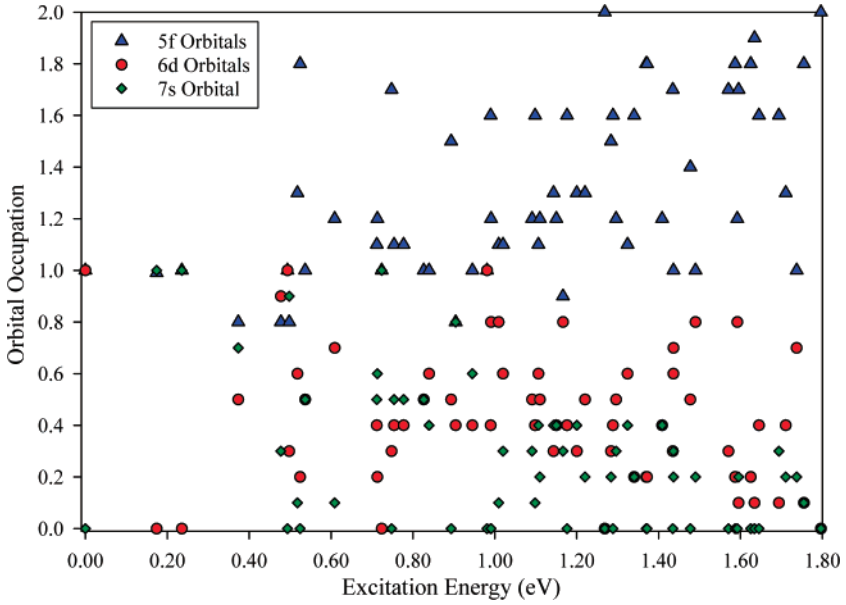

Figure 1. Calculated orbital occupancies for ground-state (0 eV) and excited-state PaO^+.

states correspond to $Th^{3+}(6d)O^{2-}$. Goncharov et al.[73] studied UO^+ by PFI-ZEKE and demonstrated that the ground state corresponds to $U^{3+}(5f^3)O^{2-}$. The low-lying states of UO^+ up to 0.65 eV originate from $U^{3+}(5f^3)O^{2-}$, with the exception of a $U^{3+}(5f^27s)O^{2-}$ state at 0.62 eV. The energy of this latter state was previously calculated by Tyagi as 0.54 eV,[74] using a level of theory comparable to that employed in the present work for PaO^+. The energetics of the bare An^{n+} (n = 0, 1, 2, 3, ...) indicate a stabilization of the 5f orbitals relative to 6d (and 7s) across the actinide series. The promotion energies for An^{3+} from their ground states to the lowest lying 6d states reveal this trend: $\Delta E\{U^{3+}[5f^3 \rightarrow 5f^26d]\} \approx 3.7$ eV; $\Delta E\{Np^{3+}[5f^4 \rightarrow 5f^36d]\} \approx 4.7$ eV; $\Delta E\{Pu^{3+}[5f^5 \rightarrow 5f^46d]\} \approx 5.8$ eV; etc.[28] Accordingly, from the PFI-ZEKE results for UO^+,[71,73] it can be confidently assumed that the ground and low-lying states of transuranic AnO^+ correspond to $An^{3+}(5f^n)O^{2-}$, where all of the valence electrons remaining at the actinide metal centers reside in orbitals of predominantly 5f character.

Spectroscopic studies of the electronic structure of PaO^+ have not been reported. Using the formal ionic nomenclature employed for ThO^+ and UO^+, the ground state of PaO^+ calculated here (Table 5) is $Pa^{3+}(5f6d)O^{2-}$. As is evident from Figure 1 (and the full computational results; see the Supporting Information), all electronic configurations of PaO^+ up to 1.8 eV have a 5f orbital occupancy of at least 0.8. The dominant excitations at low energies correspond to 6d → 7s. At energies above ~0.5 eV the 5f occupation generally increases, i.e., 6d → 5f and 7s → 5f, with several states in the 0.5−1.8 eV range having 5f occupancies of 1.5−2. The configuration of the state at the highest energy of the calculations corresponds to $Pa^{3+}(5f^2)O^{2-}$ at 1.80 eV.

The ground and first excited states, and energies, for bare An^{3+} are[28] $Th^{3+}(5f) \rightarrow Th^{3+}(6d)$/1.14 eV, $Pa^{3+}(5f^2) \rightarrow Pa^{3+}$-(5f6d)/2.5 ± 0.9 eV, and $U^{3+}(5f^3) \rightarrow U^{3+}(5f^26d)$/3.7 ± 0.7 eV. The ground and first excited states, and energies, for the corresponding AnO^+ are $Th^{3+}(7s)O^{2-} \rightarrow Th^{3+}(6d)O^{2-}$/0.36 eV,[71,72] $Pa^{3+}(5f6d)O^{2-} \rightarrow Pa^{3+}(5f7s)O^{2-}$/0.17 eV (calculated, this work), and $U^{3+}(5f^3)O^{2-} \rightarrow U^{3+}(5f^27s)O^{2-}$/0.62 eV.[71,73] Compared with the bare An^{3+}, the 5f energies of the $An^{3+}O^{2-}$ increase relative to the 6d/7s energies. In contrast to $Th^{3+}(7s)O^{2-}$ and $Pa^{3+}(5f6d)O^{2-}$, for $U^{3+}(5f^3)O^{2-}$ the 5f destabilization is smaller than the difference between the 5f and 6d/7s energy. This results in U^{3+} and $U^{3+}O^{2-}$ both having $5f^3$ ground states; however, the energy of the $5f^2$ excited state is much lower for $U^{3+}O^{2-}$ than for U^{3+}. For both Pa^{3+} and $Pa^{3+}O^{2-}$, the 6d level lies below the 7s. For Th^{3+} and U^{3+}, like Pa^{3+}, the 6d level is below the 7s; however, for $Th^{3+}O^{2-}$ and $U^{3+}O^{2-}$ the 7s is below the 6d. Thus, a 6d/7s energy inversion evidently appears with ThO^+ and UO^+, but not with PaO^+.

Comparative Reactivities of Metal Monoxide Ions with Alkanes and Alkenes. The results in Table 2 indicate disparate reactivities of the early AnO^+ ions (An = Th through Np), as has been briefly discussed elsewhere.[75] The four transuranic actinide monoxide ions, NpO^+, PuO^+, AmO^+, and CmO^+, were each inert toward the studied hydrocarbons, within the detection limit. With the exception of the radical-like $ThOC_3H_5^+$ product, the other products in Table 2 correspond to elimination of one or two H_2 molecules or of a closed-shell hydrocarbon. For PaO^+ and TaO^+, the reactivities largely parallel those of the corresponding bare M^+ and are indicative of oxidative insertion of the metal center of the MO^+ into a C−H or C−C bond. As is seen from the results in Table 2, the ordering of reactivities is as follows (the four inert transuranic AnO^+ cannot be differentiated based on the present results):

$$TaO^+ > PaO^+ \gg ThO^+ > UO^+ > (NpO^+, PuO^+, AmO^+, CmO^+)$$

The dominant $ThOC_3H_5^+$ product of the ThO^+/C_4H_8 reaction is indicative of radical-like attack on 1-butene, rather than oxidative insertion. The high efficiency of TaO^+ at hydrocarbon activation by oxidative insertion is consistent with its $Ta^{3+}(5d6s)O^{2-}$ $^3\Delta$ electronic configuration,[76] which has two unpaired valence electrons at the metal center to enable facile C−H bond activation by oxidative insertion. The appearance of double-dehydrogenation channels for TaO^+ indicates that the Ta metal

(73) Goncharov, V.; Kaledin, L. A.; Heaven, M. C. *J. Chem Phys.* **2006**, *125*, 133202.

(74) Tyagi, R. Ph.D. Thesis, Ohio State University, 2005.

(75) Gibson, J. K.; Haire, R. G.; Marçalo, J.; Santos, M.; Leal, J. P.; Pires de Matos, A.; Tyagi, R.; Mrozik, M. K.; Pitzer, R. M.; Bursten, B. E. *Eur. Phys. J. D* **2007**, in press (published online May 4, 2007).

(76) Dyke, J. M.; Ellis, A. M.; Fehèr, M.; Morris, A.; Paul, A. J.; Stevens, J. C. H. *J. Chem. Soc., Faraday Trans. 2* **1987**, *83*, 1555−1565.

center retains a reactive configuration in the initial H_2-elimination products; evidently the interaction of the cationic metal center of TaO^+ with the π-electron system of the nascent alkene or alkyne product does not render it inert toward further bond activation of the hydrocarbon ligand(s).

The reactivity of UO^+ toward the hydrocarbons was minimal. Inefficient dehydrogenation of 1-butene was observed for UO^+, but not for NpO^+, PuO^+, AmO^+, or CmO^+. Cornehl et al.[30] reported a similar reactivity of UO^+ with 1-butene and a contrasting inert behavior for its 4f homologue, NdO^+. This distinction was considered to indicate participation of the 5f electrons of $U^{3+}(5f^3)O^{2-}$ in bond activation, while the 4f electrons of $Nd^{3+}(4f^3)O^{2-}$ are contrastingly inert.[30] With the proviso that the observed reactivity of UO^+ may be due to the existence of a low-lying (0.62 eV[71,73]) $U^{3+}(5f^27s)O^{2-}$ excited state, the present results for UO^+ and transuranic AnO^+ can be similarly taken to indicate participation of the 5f electrons of $U^{3+}(5f^3)O^{2-}$ and contrasting inert character of the 5f electrons for the later AnO^+, presumably $An^{3+}(5f^n)O^{2-}$ (An = Np, Pu, Am, Cm). The expected diminution in participation of 5f electrons in σ-type organometallic bond formation upon proceeding across the actinide series is apparent from the decrease in AnO^+/1-butene reaction efficiencies between UO^+ and NpO^+.

The results for PaO^+ with the hydrocarbons indicate a distinctively high reactivity for this particular AnO^+ (Table 2). The observed reaction channels correspond to elimination of one or two H_2 molecules, as well as elimination of CH_4 from C_3H_6, each of which is a characteristic pathway of activation by oxidative insertion, with striking similarities to the reactivity of Pa^+. The PaO^+ ion is somewhat less reactive than $Ta^{3+}(5d7s)O^{2-}$, but significantly more reactive than $U^{3+}(5f^3)O^{2-}$ and the transuranic AnO^+, which are presumed to exhibit $An^{3+}(5f^n)O^{2-}$ ground and low-lying states. From the electronic structure calculations (Table 5 and Figure 1), the ground-state configuration of PaO^+ is $Pa^{3+}(5f6d)O^{2-}$ and all excited states up to at least 1.8 eV have a 5f orbital occupation of ≥ 0.8. Accordingly, the high reactivity of PaO^+ toward small alkanes and alkenes via an oxidative insertion mechanism requiring formation of two σ-type bonds indicates substantial participation of 5f electrons in this bonding. Although the minor reactivity of UO^+ with 1-butene may indicate some 5f participation, the reactivity of PaO^+ toward this and other hydrocarbon molecules indicates a particularly substantial 5f participation for $Pa^{3+}(5f6d)O^{2-}$. This enhancement in the participation of 5f electrons in covalent bond formation for PaO^+ confirms the observations for bare Pa^+, and although such importance of 5f electrons early in the actinide series may be expected,[14] it appears that it is only with Pa that such an effect is clearly observed.

Comparative Reactivities of Metal Monoxide Ions with Dienes. The reactivity results for PaO^+ and TaO^+ with 1,3-butadiene (C_4H_6) and isoprene (C_5H_8) (Table 3) can be compared with previously reported results for LnO^+ [31] and other AnO^+.[40] According to a model developed by Cornehl et al.[31] for LnO^+/diene reactions, those LnO^+ ions having strong or moderately strong Ln^+-O bonds react with these small conjugated dienes not by direct oxidative insertion, as the valence electrons are engaged in the $Ln^+{=}O$ bond, but rather by an indirect multicentered mechanism involving electrophilic attack on the π-electron system. This model apparently also explains the reactivities of UO^+, NpO^+, PuO^+, and AmO^+ toward dienes.[40] This indirect mechanism involves the oxygen atom of the MO^+ and retains the metal center in a formally trivalent oxidation state. The product distributions and reaction efficiencies for this type of mechanism correlate with the electrophilicities of the LnO^+ or AnO^+, which are indicated by the ionization energies of the neutral oxides. The reaction efficiencies of LnO^+ and AnO^+ toward dienes thus increase in parallel with increasing IE[MO] (M = Ln, An).[31,40] The ThO^+ ion exhibited a different type of reactivity from other AnO^+.[40] For the MO^+/C_5H_8 reactions where M = Tb, Gd, Dy, Ho, Er, U, Np, Pu, or Am, the products $MOC_3H_4^+$, $MOC_5H_6^+$, and/or $MOC_5H_8^+$ all incorporate closed-shell hydrocarbons. For the ThO^+/C_5H_8 reaction, the appearance of $ThOC_5H_5^+$ is indicative of radical-like behavior, consistent with the $Th(7s)O^+$ electronic structure, which can be represented as the radical, $^\bullet ThO^+$.

The products of the efficient TaO^+/diene reactions (Table 3) are distinct from those described above. Both the TaO^+/C_4H_6 and TaO^+/C_5H_8 reactions are dominated by double dehydrogenation to give mainly $TaOC_4H_2^+$ (65%) and $TaOC_5H_4^+$ (75%), respectively. These are the same pathways that dominate for the corresponding reactions of bare Ta^+ and reveal a type of behavior reminiscent of the reactions of TaO^+ with 1-butene and *n*-butane (see Table 2). The interpretation is that TaO^+ ($Ta^{3+}(5d6s)O^{2-}$ [76]) activates the dienes primarily via a direct oxidative insertion mechanism, resulting in multiple H_2 loss, which is not a characteristic reaction pathway for indirect electrophilic attack. The different products observed in a previous study of the TaO^+/1,3-butadiene reaction probably reflect different experimental conditions.[45]

As in the case of Ta, for the PaO^+/diene reactions (see Table 3) the product distributions are basically similar to those found for Pa^+: the two products of the PaO^+/C_4H_6 reaction, $PaOC_2H_2^+$ and $PaOC_4H_4^+$, correspond to the dominant reaction pathways seen for Pa^+, whereas for the PaO^+/C_5H_8 reaction, the dominant product, $PaOC_3H_4^+$, also corresponds to the major product in the Pa^+/C_5H_8 reaction. The high reaction efficiencies observed in both PaO^+/diene reactions, essentially similar to the efficiencies obtained for bare Pa^+ and Ta^+, as well as for TaO^+, are a confirmation of the distinctively high reactivity of PaO^+, which is interpreted as a manifestation of an oxidative insertion mechanism with dienes. The UO^+, NpO^+, PuO^+, and AmO^+ ions were all inert toward C_4H_6, and the ThO^+ ion formed the association complex only in an inefficient way, while Th^+, U^+, and Np^+ were very reactive with this substrate.[40] The ThO^+, UO^+, NpO^+, PuO^+, and AmO^+ ions were all reactive with C_5H_8 but with very low efficiencies compared to PaO^+, whereas Th^+, U^+, and Np^+ were very reactive.[40]

In conclusion, this assessment of the reactions of PaO^+ with 1,3-butadiene and isoprene suggests that the reactivity is dominated by an oxidative insertion mechanism, akin to that observed in the case of alkanes and alkenes. This constitutes a confirmation of the active role played by the 5f electrons of PaO^+ in its reactivity with hydrocarbons.

Summary and Conclusions

Systematic FTICR/MS studies have been carried out of gas-phase reactions of bare and oxo-ligated actinide cations, An^+ and AnO^+ where An = Th, Pa, U, Np, Pu, Am, or Cm, with alkanes and alkenes (CH_4, C_2H_6, C_3H_8, *n*-C_4H_{10}, C_2H_4, C_3H_6, and 1-C_4H_8). With the exception of the unreactive Am^+ ion, each of the An^+ ions activated one or more of the hydrocarbons by an oxidative insertion mechanism that proceeded via an activated intermediate characterized as having $\{C-An^+-H\}$ or $\{C-An^+-C\}$ bonding. The following order of reactivities was established: $Th^+ > Pa^+ > U^+ > Np^+ > Cm^+ > Pu^+ > Am^+$. The high reactivity of Th^+ is tentatively attributed to its quartet $6d^27s$ configuration;[23,28] its behavior is characteristic of a d-block transition metal ion.[52,54] The reactivities of Cm^+, Pu^+, and Am^+

correlate with the excitation energies to provide $5f^{n-2}6d7s$ states suitable for bond insertion, which indicates that their 5f electrons are not involved in oxidative insertion. As Pa^+, U^+, and Np^+ each have a ground state, or very low-energy ($\Delta E \leq 0.1$ eV) $5f^{n-2}6d7s$ configuration,[28] their distinctly different reactivities are attributed to a decrease in 5f participation from Pa^+ to U^+ to Np^+. The results suggest substantial participation of the 5f electrons of Pa^+ in σ-type organometallic bonding.

Among the seven studied AnO^+ ions, only ThO^+, PaO^+, and UO^+ exhibited reactivity with one or more alkanes or alkenes; the reactivity of PaO^+ was distinctively high. Reactions of PaO^+ with butadiene and isoprene were studied for comparison with results for LnO^+ ions[31] and other AnO^+ ions.[40] Apparently, as with the alkanes and alkenes, PaO^+ activates these dienes primarily by an oxidative insertion type of mechanism. Comparative studies performed with TaO^+ and these same substrates confirm this interpretation. The reactivity of ThO^+ is not indicative of oxidative insertion but rather of radical-like behavior, as expected from its electronic structure, $Th^{3+}(7s)O^{2-}$.[72] The ground state and low-lying states of UO^+ correspond to $U^{3+}(5f^3)O^{2-}$.[73]

The electronic structure of PaO^+ is reported here for the first time from electronic structure calculations. The ground state of PaO^+ was found to be $Pa^{3+}(5f6d)O^{2-}$. All excited states up to 1.8 eV were found to have a 5f orbital occupation of ≥ 0.8 electron. The high reactivity of PaO^+ is only moderately less than that of $Ta^{3+}(5d6s)O^{2-}$. Thus, given the substantial 5f character of the ground and low-lying excited states of PaO^+, these results indicate significant participation of the 5f electrons of the oxo-ligated protactinium metal center in oxidative insertion.

The reactivities of Pa^+ and, more so, of PaO^+, reported here, reveal a distinctive role of the 5f electrons in σ-type organoprotactinium bond formation and are, to the best of our knowledge, the first clear experimental evidence, that is supported by theory, of the active role of 5f electrons in this type of actinide chemistry. These gas-phase ion chemistry results suggest that substantial 5f participation in σ-bonded organoactinide chemistry might also appear for Pa in the condensed phase, in contrast to Th and U.[77] Complications associated with handling radioactive Pa-231—alpha decay, half-life = 32 800 y, with several short-lived radioactive progeny—seriously hampers progress in the condensed-phase organometallic chemistry of this pivotal member of the actinide series.

Acknowledgment. The work has been sponsored by the U.S. Department of Energy, Office of Basic Energy Sciences, under contracts DE-AC05-00OR22725 (ORNL), DE-FG02-01ER15136 (OSU), and DE-FG02-01ER15135 (UT), and by Fundação para a Ciência e a Tecnologia (FCT) and POCI 2010 (cofinanced by FEDER) under contract POCI/QUI/58222/2004. M.S. is grateful to FCT for a Ph.D. grant. We thank R. Tyagi for an exploratory calculation on PaO^+.

Supporting Information Available: The calculated energies, orbital occupations, and contributing terms for the 63 electronic states of PaO^+ from ground up to 1.8 eV are tabulated. This information is available free of charge via the Internet at http://pubs.acs.org.

OM700329H

(77) Cotton, S. *Lanthanide and Actinide Chemistry*; Wiley: Chichester, 2006.